Biochimica et Biophysica Acta 1817 (2012) 1490–1498

Contents lists available at SciVerse ScienceDirect

Biochimica et Biophysica Acta

journal homepage: www.elsevier.com/locate/bbabio

Drought-induced modifications of photosynthetic electron transport in intact leaves: Analysis and use of neural networks as a tool for a rapid non-invasive estimation ☆

Vasilij Goltsev [a], Ivelina Zaharieva [b], Petko Chernev [b], Margarita Kouzmanova [a], Hazem M. Kalaji [c,*], Ivan Yordanov [a], Vassilena Krasteva [a], Vladimir Alexandrov [a], Detelin Stefanov [a], Suleyman I. Allakhverdiev [d,e], Reto J. Strasser [f]

[a] Department of Biophysics and Radiobiology, Faculty of Biology, St. Kliment Ohridski University of Sofia, 8, Dragan Tzankov Boulevard, 1164 Sofia, Bulgaria
[b] Freie Universität Berlin, Arnimallee 14, 14195 Berlin, Germany
[c] Department of Plant Physiology, Warsaw University of Life Sciences SGGW, Nowoursynowska 159, 02-776 Warsaw, Poland
[d] Institute of Plant Physiology, Russian Academy of Sciences, Botanicheskaya Street 35, Moscow 127276, Russia
[e] Institute of Basic Biological Problems, Russian Academy of Sciences, Pushchino, Moscow Region 142290, Russia
[f] Bioenergetics Laboratory, University of Geneva, CH-1254 Jussy/Geneva, Switzerland

ARTICLE INFO

Article history:
Received 31 January 2012
Received in revised form 25 April 2012
Accepted 28 April 2012
Available online 15 May 2012

Keywords:
Artificial neural network
Delayed fluorescence
Drought stress
JIP-test
Prompt fluorescence
Reflection change at 820 nm

ABSTRACT

Water deficit is one of the most important environmental factors limiting sustainable crop yields and it requires a reliable tool for fast and precise quantification. In this work we use simultaneously recorded signals of photoinduced prompt fluorescence (PF) and delayed fluorescence (DF) as well as modulated reflection (MR) of light at 820 nm for analysis of the changes in the photosynthetic activity in detached bean leaves during drying. Depending on the severity of the water deficit we identify different changes in the primary photosynthetic processes. When the relative water content (RWC) is decreased to 60% there is a parallel decrease in the ratio between the rate of excitation trapping in the Photosystem (PS) II reaction center and the rate of reoxidation of reduced PSII acceptors. A further decrease of RWC to 20% suppresses the electron transfer from the reduced plastoquinone pool to the PSI reaction center. At RWC below values 15%, the reoxidation of the photoreduced primary quinone acceptor of PSII, Q_A^-, is inhibited and at less than 5%, the primary photochemical reactions in PSI and II are inactivated. Using the collected sets of PF, DF and MR signals, we construct and train an artificial neural network, capable of recognizing the RWC in a series of "unknown" samples with a correlation between calculated and gravimetrically determined RWC values of about $R^2 \approx 0.98$. Our results demonstrate that this is a reliable method for determination of RWC in detached leaves and after further development it could be used for quantifying of drought stress of crop plants *in situ*. This article is part of a Special Issue entitled: Photosynthesis Research for Sustainability: from Natural to Artificial.

1. Introduction

Drought stress, together with high temperature and high salinity, is one of the main stress factors that influence the development and productivity of plants [1–7]. Plants have developed various strategies to eliminate or partially decrease the negative impacts of drought [8–10], such as: "escape" from the dry period by fast vegetative growth; "dehydration avoidance" by retaining water in the tissues or; development of physiological "tolerance" to drought [11]). Drought resistance is typically based on increased activity of antioxidant enzymes [12], and changes in plant morphology, anatomy, physiology and biophysics [13–15]. Understanding the complex physiological, biochemical, biophysical and molecular basis of stress tolerance in plants is not only an important theoretical problem in ecology and environmental science, but also has practical applications in resolving agricultural problems and increasing crop yield [16].

Abbreviations: ANN, artificial neural network; DF, delayed fluorescence; F_M and F_0, maximum and minimum fluorescence intensity during the induction period; J and I, intermediate steps in the chlorophyll *a* fluorescence rise (OJIP) appearing between F_0 and F_M at about 3 and 30 ms, respectively; MR, modulated light reflection at 820 nm; NIR, near infra-red; OEC, oxygen evolving complex; P680 and P700, the chlorophyll molecules of PSII and PSI reaction center respectively; PCA, principal component analysis; PF, prompt fluorescence; PSI (II), photosystem I (II); PQ, oxidized plastoquinone; Q_A and Q_B, primary and secondary quinone electron acceptors of PSII; RC, reaction center; RWC, relative water content in leaves

☆ This article is part of a Special Issue entitled: Photosynthesis Research for Sustainability: from Natural to Artificial.

* Corresponding author. Tel.: +48 608079998; fax: +48 226425923.
E-mail address: hazem@kalaji.pl (H.M. Kalaji).

0005-2728/$ – see front matter © 2012 Elsevier B.V. All rights reserved.
doi:10.1016/j.bbabio.2012.04.018

Quantifying the degree of drought stress experienced by plants is essential for studying drought tolerance and is typically based on the measurement of indicators such as leaf water potential and relative water content (RWC) [17]. RWC is expressed as a percentage of the maximum water content that a plant tissue is capable of retaining [18]. RWC is considered to be the best criterion for plant water status [19]. The optimal water content at non-stress conditions is RWC between 80% and 90% since at this level no changes in the normal plant physiology can be detected [20]. However, when RWC falls below 70% (the so-called mild drought stress, which is one of the most common stress conditions in nature [21]), a cascade of physiological processes is initiated with negative impacts for the plant. These changes include turgor loss, decrease in leaf water potential, stomatal closure and decrease in internal CO_2 concentration [22,23], all of which can lead to impairment of photosynthetic activity [24]. When the drought stress is accompanied with high light, the down regulation of photosynthesis causes an energy imbalance in the PSII reaction center (RC) leading to molecular oxygen photoreduction [25] and photoinhibition [26]. The typical results of oxidative stress reactions in leaf tissue are pigment photo-oxidation, chlorophyll degradation and chlorophyll synthesis deficiency [27], all of which can be regarded as protective mechanisms to minimize light absorption by chloroplasts [26]. Rascio and La Rocca [28] identified three types of events in plant cells which are induced by desiccation: membrane damage, mechanical stress, and oxidative stress. Water removal induces cell shrinkage, increase of the cytoplasm viscosity and cell wall folding which result in membrane destruction and protein denaturation [29]. Extracellular hydrolases penetrate into the cell, which ultimately leads to cell death. To maintain their functionality the plant cells respond by accumulating of sugars and a specific class of hydrophilic proteins known as *LEA-proteins* (late embryogenesis abundant) [30]. These proteins stabilize cell membranes, support the hydration shell thereby preventing protein aggregation and promote subcellular vitrification [31]. This results in slowly reversible or irreversible damage to the photosynthetic apparatus [32,33]. However, according to our best knowledge the correlation between these effects and RWC has not been yet quantified.

Determination of the RWC parameter is clearly important for estimating the physiological state of plants subjected to water stress, but quantification by traditional methods is slow (often >24 h) because of the time needed for drying or water equilibration [34,35]. There are faster commonly used techniques to measure remotely the water status of individual plants or canopies based on infrared thermography or thermal infrared imaging. With infrared thermography the leaf or canopy temperature is measured which directly correlates with transpiration rate and stomatal conductance [36,37]. These parameters are indirectly related to the leaf water content.

A more direct correlation is found between near infra-red (NIR)-based stress indices and the RWC of leaves, although this correlation has so far only been observed in severely drought-stressed samples [38,39]. NIR imaging analysis of water stress in plants is based on absorption by water present in the leaves, with characteristic water absorption bands at 1450 nm, 1930 nm, and 2500 nm [40]. The disadvantage of NIR-based methods is not only their low sensitivity [11] but also that they more likely reflect an overall change in plant and canopy architecture with the reduction of the biomass and foliar density associated with the water deficit rather than reflecting the real decrease in the relative water content [40].

A rapid, automated and non-destructive method for quantification of leaf water content is therefore highly desirable, especially since effective growth management often requires continuous real-time *in situ* monitoring. A possible approach to develop such a method is to explore the native physiological response of plants to water stress. Such an approach should be based on a fast, sensitive and easy to measure signal which should be correlated and calibrated to RWC. A good candidate for such a method is the chlorophyll prompt fluorescence (PF) emitted from the leaves, as it has already been used as a very sensitive tool for monitoring the changes in the physiological status [41]. An especially valuable tool for screening of photosynthetic performance is the measurement of fluorescence induction kinetics (Kautsky phenomenon) [42,43]. There are many examples of the use of numerical parameters of these induction curves to monitor the physiological response of plants to different stressors, for example: photoinhibition of photosynthesis [44], herbicide effects [45], biostress effects [46,47], and water stress [48–55]. Due to the high sensitivity of the fluorescence induction curves to different stress effects, highly sophisticated models such as the JIP test have been developed [56,57] allowing rapid screening and modeling of plant stress response [1,2,57–61]. Moreover it has been shown that the drought stress response of plants is closely related to changes in photosynthetic activity [21,32,33], which is monitored by the JIP test.

The JIP-test equations are based on the theory of energy fluxes in biomembranes [62]. The JIP-test parameters link the different steps and phases of the PF transient with the redox states of PSII and respectively with the efficiencies of electron transfer (in the intersystem chain and to the terminal electron acceptors at the PSI acceptor side). This makes it a potentially valuable tool for estimating the effects of water scarcity on photosynthetic electron transport. Moreover, the relationship between fluorescence data and some biochemical and physiological parameters under drought conditions have been demonstrated by modern statistical procedures such as stepwise regression, factor analysis, cluster analysis, and principal component analysis [24,63,64].

Although the basic pattern of the Kautsky curve [42] is similar in all plants, species-specific differences in trajectory of fluorescence intensity plotted over time allow PF induction curves to be used a "fluorescence fingerprint" to identify plant species [65,66]. PF induction curves have already been parameterized and further pattern recognition procedures involving the use of different types of artificial neural networks (ANN) for grouping of time traces or numerical fluorescence parameters have been successfully applied [67]. As it is difficult to define a single robust criterion based on the fluorescence induction curve, using the neural networks can result in better sensitivity of fluorescence measurements to the potential damages induced by water scarcity.

In this study we analyze the desiccation induced modifications in different sites of the photosynthetic electron transport chain in detached bean leaves. In order to get more information about the processes in leaves caused by decreased water content and to develop a more complex, stable and reliable method for RWC estimation, in addition to recording of PF curves, we simultaneously monitor two other different signals that give complementary information about the photosynthetic apparatus: delayed chlorophyll fluorescence (DF), and modulated light reflection (MR) at 820 nm. The DF fluorescence curves give information about the redox reactions in PSII [58,68,69]. The MR signal measured at 820 nm provides information about electron transport after the plastoquinone (PQ) and to the PSI acceptors [58,70]. In this work, we design artificial neural networks based on the simultaneous registration of PF, DF and MR signals to develop a useful tool for rapid, not-invasive automatic determination of RWC in leaves subjected to desiccation.

2. Material and methods

2.1. Plant material

Bean plants (*Phaseolus vulgaris* cv. Cheren Starozagorski) were grown on fertilized soil mixture in a chamber at controlled temperature (22–23 °C), light (250 μmol photons m^{-2} s^{-1}), and humidity (60–65%) at photoperiod 12/12 h. 10 days old plants were decapitated by removing the stem, buds, apex and the newly appearing leaves

just above the already formed leaves as in Yordanov et al. [71]. Well-formed primary leaves of 20–25 days old decapitated plants were used in the experiments.

2.2. Leaf drying and RWC estimation

To quantify the influence of desiccation, we performed the following sequence of measurements: 1) each leaf was detached and fully hydrated by submerging the leaf under water for several minutes; after removing the residual moisture on the surface the weight M_t, corresponding to 100% RWC, was measured. 2) each leaf was dried at 22 °C at 40–45% air humidity during a 45 h period; at different moments of desiccation (0.5, 1, 1.5, 2, 3, 4, 6, 8, etc. 45 h) the PF, DF and MR signals were simultaneously recorded; immediately after that the weight M_f was measured; 3) the leaf was dried in an oven and the weight M_d, corresponding to 0% RWC, was measured. The watering and drying were conducted in dim ambient light (<<1 μmol photons m^{-2} s^{-1}).

Three independent experiments were conducted. In each experiment 12 matured leaves with approximately same size (chosen from 30 bean plants) were detached. In each leaf 3 measurements of photosynthetic activity of different spots were taken producing a total of 108 repetitions for each drying step.

The relative water content at different stages of drying was determined by the gravimetric method [18] using the equation

$$RWC\% = 100\left(M_f - M_d\right)/(M_t - M_d) \quad (1)$$

For each individual leaf M_t was determined by measuring the weight after watering, M_f was measured at different stages of drying immediately after measuring of PF, DF and MR induction curves, and M_d was determined after drying in oven at 104 °C (until a constant mass is reached).

2.3. Evaluation of photosynthetic activity

Induction kinetics of PF, DF and MR were simultaneously recorded using a Multifunctional Plant Efficiency Analyzer, M-PEA (Hansatech Instrument Ltd., King's Lynn, Norfolk, PE30 4NE, UK) as described in [52,58,60]. The watering and drying of the leaves were done at very low light, so we assumed that all leaves were dark-adapted before the measurements of the induction curves. Measurements were conducted for an induction period of 1 s. Leaves were illuminated by red light of 2000 μmol m^{-2} s^{-1} PPFD. The JIP test parameters and the numerical processing of the PF, DF, and MR signals were performed by the in-house software M-PEA data Analyzer v.5.1 [58].

2.4. Neural network training and testing

Artificial neural networks were developed using the MatLab (v. 6.5) software. The networks were feed forward, with hyperbolic tangent sigmoid transfer function in the hidden layer and a linear transfer function in the output layer [72,73]. Three or four neurons were used in the hidden layer. An error back propagation method with Bayesian regularization algorithm [74] was used for network training. In total, 1184 PF, DF, and MR signal datasets were used for training and testing. The experimental data was not directly presented to the inputs of the network. Instead, principal component analysis (PCA) was performed on the input data, and only the principal components whose contribution to the total variation was larger than 0.05% were selected as inputs to the network. The number of principal components that were used thus varied depending on the type of input data. Correlation coefficients (or regression R-values) (R^2), and standard deviations (SD) were used to estimate the performance of the ANN.

3. Results

We used detached primary leaves of decapitated bean plants as a model system to study the plant response to drought stress. In such leaves senescence processes are delayed and they are able to maintain a stable physiological state over several weeks [71], making them a stable experimental system to study the effects of progressive drying in laboratory conditions. The protocol we used for desiccation allowed us to make direct correlation between the level of desiccation (calculated as RWC) and the photosynthetic activity (estimated from the PF, DF and MR signals as described further below). In a control experiment we verified that the leaf detachment does not cause a change in the measured parameters (see Supplementary data).

3.1. Photosynthetic activity at different levels of drought stress

Prompt chlorophyll fluorescence, delayed fluorescence and MR absorption changes are considered to be sensitive indicators for water stress in intact leaves [58]. We found that progressive desiccation (i) decreased the signal amplitudes and (ii) modified the shape of the induction curves for all three signals (Fig. 1).

During the initial stages of desiccation, *the intensities* of both PF and millisecond DF were almost unaffected until the RWC reached about 20%. When the water content was decreased below 20%, the intensity of both PF and DF sharply decreased. In a clear contrast to the overall intensity, *the shape* of the DF induction curve is sensitive to water stress in the initial stages of drought stress (Fig. 1B). In the range of RWC between 100 and 50% the characteristic peak in the DF induction curve (I_2) disappears. The MR signal, similar to PF, remained almost unaffected by the decreased water content until a level of 30% RWC was reached (Fig. 1C). However, between 30% and 4% the slow increase of the signal, which normally starts after 20 ms of illumination, was absent. Desiccation below 4% affects not only the slow increase, but also the fast decrease in intensity observed during the first milliseconds of illumination.

In order to get further insights into the mechanisms underlying the observed changes, we applied the JIP test model [57,58] to the induction curves of PF. The effects of desiccation on photosynthetic electron transport were estimated from several JIP test parameters (presented as a spider plot graph in Fig. 2A). The spider plot graphically represents the drought induced modification in the photosynthetic machinery. Each level of drought is represented by a dodecagon with corners corresponding to the relative (to the values of fully hydrated leaf) JIP parameters. The selected parameters are:

a) quantum yields of photoinduced electron transport in PSII reaction center to Q_A (φ_{Po}), from Q_A^- to plastoquinone (φ_{Eo}), or from PQ to terminal acceptors of PSI (φ_{Ro});
b) efficiency/probability that the electron reaches electron carriers after Q_A^- (ψ_{Eo}), or that the electron is transferred from the intersystem electron carriers to the electron acceptors at the PSI acceptor side (δ_{Ro});
c) probability that a PSII chlorophyll molecule functions as a RC (γ_{RC});
d) approximated initial slope (in ms^{-1}) of the fluorescence transient normalized to the maximal variable fluorescence F_V (M_0);
e) absorption flux from the antenna per RC, which is a measure of PSII apparent antenna size (ABS/RC);
f) trapped energy flux (per RC) which reduces Q_A (TR_0/RC);
g) performance index (expressed in analogy to the Nernst potential) for conservation of energy of the photons absorbed by PSII in the form of reduced intersystem electron acceptors (PI_{ABS});
h) performance index (potential) for conservation of energy of the photons absorbed by PSII in form of reduced acceptors of PSI (PI_{total}).

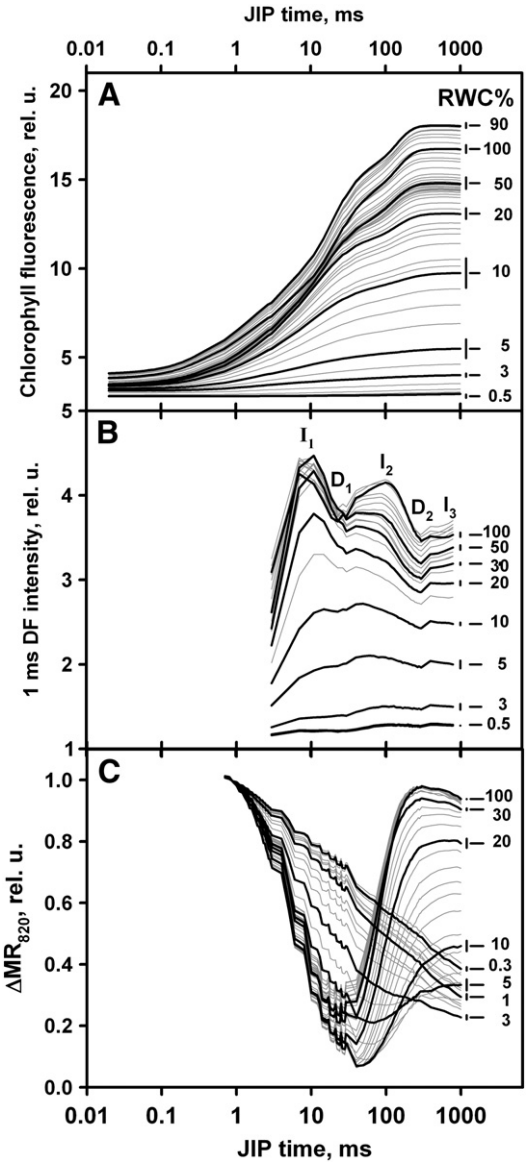

Fig. 1. Drought stress effect on the induction curves of PF (A), DF (B) and MR (C) in detached bean leaves. The MR signal was normalized to the average of the MR values recorded between 0.3 and 0.7 ms. Each induction curve was averaged from 20 curves measured in leaves with closest values of RWC. (The RWC deviation in leaf samples used for averaging did not exceeded 2%.) Some representative curves are drawn with thick lines and the corresponding mean RWC values are shown at the right side of the curves. The vertical bars near the transients show the standard error (maximal value from all points in the corresponding curve).

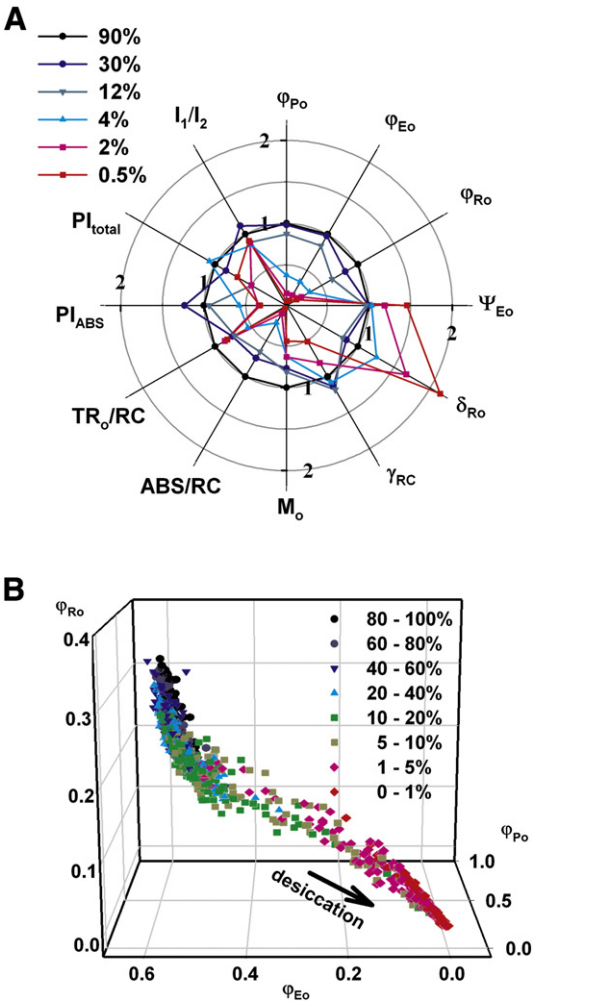

Fig. 2. JIP-test parameters and the DF parameter I_1/I_2, calculated from 1184 sets of PF and DF induction curves measured in bean leaves with different water content. (A) Spider plot presenting the parameters calculated from leaves with different RWC (see text for the meaning of the parameters). For each group, 50 measurements from leaves with similar RWC are averaged. The values are normalized to the value at 100% RWC. (B) 3D phase diagram showing the relationship between the quantum yields of photoinduced electron transfer from P680 to Q_A (φ_{Po}), from Q_A^- to plastoquinone (φ_{Eo}), and from PQ to the PSI electron acceptors (φ_{Ro}). All individual measurements are shown with different symbol and color corresponding to the different RWC.

For further details on parameter definitions see [57,58]. In addition to these parameters of PF, the ratio of the first two peaks (I_1/I_2) in the induction curve of DF is shown. This ratio was found to be inversely connected to electron flow in PSII [75].

During desiccation the parameters change in different ways to form polygons with specific shapes. In this way, the functional state of photosynthetic machinery can be visualized as a geometric figure with a shape which is specific for the drought stress. It is also sensitive to the different levels of desiccation. For this reason, we argue that the constellation of the selected parameters can be used for empirical estimation of RWC.

The three parameters plotted in Fig. 2B reflect the quantum yields of the electron transport in PSII, PSI and between them (φ_{Po}, φ_{Ro} and φ_{Eo}, correspondingly). They were highly sensitive to water stress and strongly decreased at low water content. These parameters were used to evaluate the drought stress sensitivity of different sections of the photosynthetic electron-transfer chain (Fig. 2B). The experimental points in Fig. 2B were grouped and shown in different color depending on the water stress level. The result revealed a different behavior of these parameters during desiccation. Specifically, leaves with low levels of water deficit (40–100% RWC) and strongly desiccated leaves (0–1% RWC) showed insignificant variations in the studied parameters and are grouped either in the top left corner or in the down right corner of the plot. In contrast, moderately desiccated states (1–40%) showed much higher variation in electron-transport quantum yields. Also, the desiccation-induced changes of quantum yields of electron transport from the reaction center of PSII P680 to Q_A (φ_{Po}), and from Q_A^- to PQ (φ_{Eo}) were similar, while the quantum yield of the electron transport from the reduced PQ to the PSI acceptors (φ_{Ro}) had a different behavior. Overall a rather narrow trace in 3D space was formed by all of the examined parameters. This clearly indicates the suitability of fluorescence measurements for estimation of RWC in plant leaves.

To better illustrate the changes in the three parameters reflecting the electron-transport yields at the different stages, we plotted the φ_{Po}, φ_{Eo} and φ_{Ro} as a function of RWC (Fig. 3A). The quantum yields

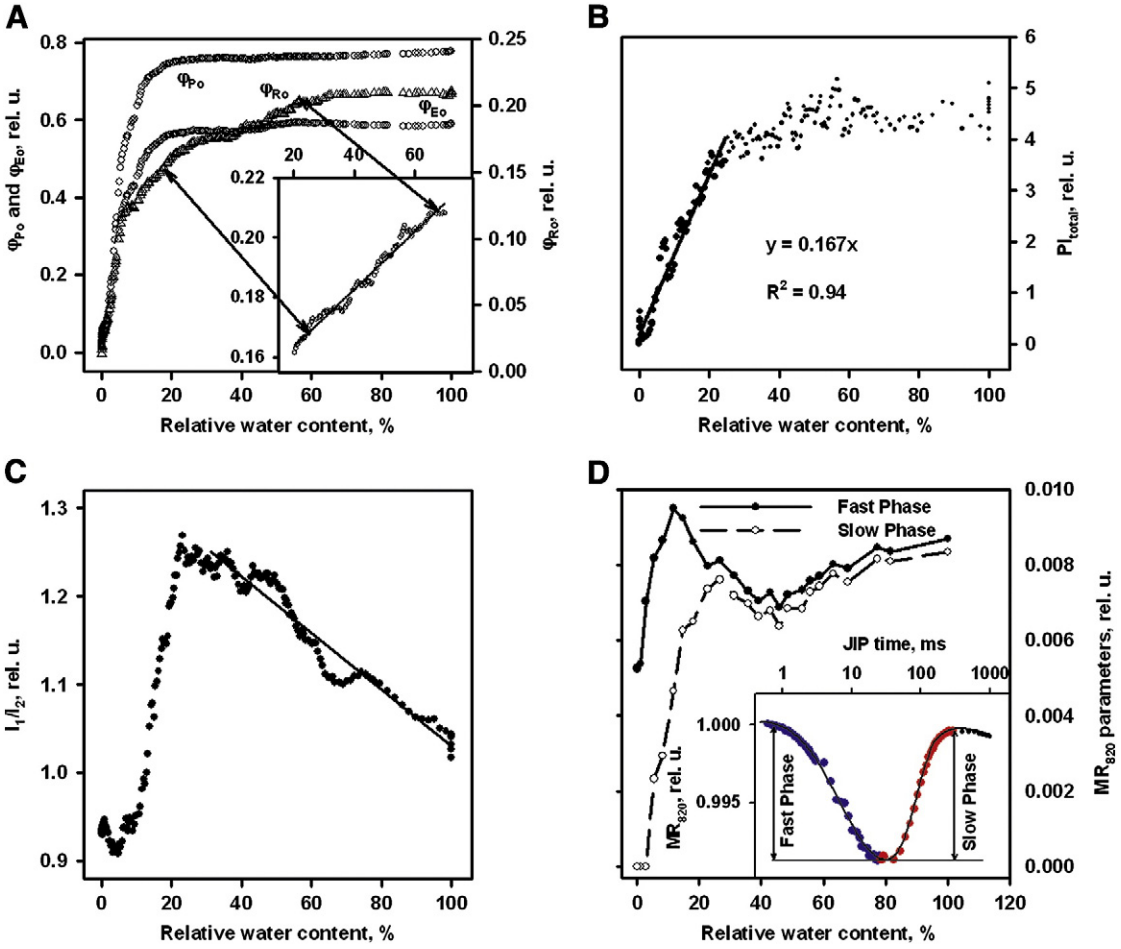

Fig. 3. Effect of RWC on the parameters calculated from PF, DF and MR induction curves. The experimental points are smoothed by "running average" algorithm with window of 50 points. (A) Quantum yield of electron transfer in PSII reaction center (φ_{Po}), at PSII acceptor side (φ_{Eo}) (left scale) and from the reduced PQ toward $P700^+$ (φ_{Ro}) (right scale). Inset: the most sensitive to RWC range for φ_{Ro}. The straight line represents the linear regression of the experimental points. (B) Total performance index (PI_{total}). The straight line represents the sector of linear dependence of PI_{total} on RWC (0÷25%). (C) Ratio between the first two peaks in the DF induction curve (I_1/I_2). The straight line shows the linear dependence of I_1/I_2 on RWC within the range 40÷100%. (D) Amplitudes of fast and slow phase of induction curve of MR. Inset: the amplitudes of the fast and slow phases are calculated subtracting the minimum of the curve from the maximum of the signal at the beginning of the illumination (fast phase) and from the maximum of the signal at the end of the illumination (slow phase).

of the primary photochemical reaction in PSII reaction center (φ_{Po}) and of electron transport in PSII acceptor side (φ_{Eo}) remained almost constant when the RWC varied between 100% and 30%, but decreased linearly with water loss between 20% and 0% RWC. The third quantum yield parameter (φ_{Ro}), which reflects the inter-system electron transport showed a different behavior at higher water content (RWC between 60% and 20%) as compared to other measured parameters. The φ_{Ro} dependence on the water content remained linear, but with a much lower slope, and strongly deviated from the dependences of φ_{Po} and φ_{Eo}. This parameter showed a very rapid change (with a slope similar to the other two parameters) only at low RWC (below 15% RWC).

Another fluorescence parameter which changed significantly during desiccation (Fig. 2A) was the performance index (PI). This is one of the chlorophyll fluorescence parameters that provides useful quantitative information about the state of plants and their vitality [1,2,60,76] and therefore can be used for the analysis of plant stress response [77]. The leaf photosynthetic activity as monitored by PI_{total} parameter seemed to be tolerant to water stress over a wide range of RWC values (100% to 30%) and decreased linearly with water loss between 20% and 0% RWC (Fig. 3B).

From the DF parameters, the I_1/I_2 ratio was found to be most sensitive to mild drought stress (Fig. 3C). A well expressed linear dependence on RWC between 100% and 40% RWC was observed (Fig. 3C). Interestingly, again an almost linear dependence but not with the same slope was observed at lower RWC: I_1/I_2 sharply decreased between 20% and 5%, and then at even lower RWC again slightly increased. We suggest that the increase at very low RWC values indicates the complete inhibition of primary photochemistry in PSII. The increase between 100% and 20% RWC reflects the deactivation of the electron flow from Q_A^- toward PQ.

The MR signal was also modified by the decreased water content. The fast phase of the signal, which corresponds to the kinetics of the photoinduced changes in the P700 redox state, was significantly modified only at RWC below 10% (Fig. 3D). The slow phase of the MR signal, which reflects $P700^+$ re-reduction, was more sensitive and decreased progressively at RWC values below 30%, disappearing completely at about 3% RWC.

3.2. Neural networks

Artificial neural networks were constructed to connect leaf water content with measured experimental data. On the input of a network, PF/DF/MR data was presented, and the network was asked to return a guess for the RWC of the corresponding sample. As inputs for the networks, we used three types of data (Table 1): i) complete induction curves of PF, DF or MR, and the combination of the three of them; ii) parameters from the JIP test: the quantum yields of photoinduced

Table 1
Input characteristics and statistical results of tested ANNs.

Type of input data	Input values	Principal components	Hidden neurons	All data		Testing population	
				R^2	SD	R^2	SD
Whole induction curves							
PF	78	7	3	0.94	7.0	0.94	6.95
			4	0.94	6.6	0.94	6.83
DF	40	30	3	0.93	7.84	0.90	8.68
			4	0.94	7.52	0.90	8.48
MR	85	61	3	0.70	15.94	0.56	19.14
			4	0.72	15.75	0.44	24.94
PF, DF, MR	203	46	3	0.96	5.44	0.96	6.35
			4	0.98	5.05	0.96	6.11
JIP parameters							
φ_{Po}, φ_{Ro}, φ_{Eo}	3	3	3	0.77	14.09	0.77	13.52
			4	0.77	13.92	0.77	13.48
δ_{Ro}, ψ_{Eo}, γ_{Rc}	3	3	3	0.86	10.94	0.85	11.24
			4	0.86	10.49	0.85	10.83
PI_{ABS}, PI_{total}	2	2	3	0.67	16.68	0.71	15.65
			4	0.67	16.67	0.69	15.68
All JIP parameters	17	3	3	0.77	14.09	0.77	13.52
			4	0.77	13.94	0.77	13.32
DF induction parameters							
I_1, I_1/I_2	2	2	3	0.88	14.15	0.87	13.97
			4	0.88	13.95	0.87	13.92

electron transport reaction at different parts of the electron transport chain (φ_{Po}, φ_{Eo} and φ_{Ro}); the efficiencies of electron transport (δ_{Ro} and ψ_{Eo}) together with the relative concentration of the reaction center chlorophyll (γ_{Rc}); performance indexes (PI_{ABS} and PI_{total}); iii) DF parameters: the amplitude of the first peak and the ratio between the first and the second peak in the DF induction curve (I_1 and I_1/I_2).

From the total of 1184 pairs of input/output data, 888 pairs (75%) were randomly selected for network training. The remaining 296 data pairs (25%) were used to test how well the network had learned to predict the RWC from the PF/DF/MR data. The accuracy of the network was quantified by the correlation coefficient (R^2) [78] and by the standard deviation (SD) between measured and predicted RWC.

The optimum number of neurons was determined based on the minimum value of mean standard error of the training and prediction set. The optimization was performed varying the neuron number in the range 2 to 6. The best results were generated for 3 and 4 neurons (see Table 1 — other data are not shown).

The results from the training and testing of the networks for the different input data are shown in Table 1. When the complete induction curves were used as network inputs, the ANNs performed robustly for both the PF curve ($R^2 = 0.94$ for the testing data set) and the DF curve ($R^2 = 0.90$). Seemingly, the MR traces did not contain enough information for the prediction of RWC (R^2 only 0.56 with unknown data). However, when a network was trained with all three signals together, the predictions of the network were further improved ($R^2 = 0.96$). Fig. 4 shows a comparison between experimental RWC values and the values predicted using the neural network model.

When a network was trained with the JIP test parameters or with DF induction parameters, the predictions made by the network were generally not accurate. The best correlation between measured and predicted RWC was found with the DF parameters I_1 and I_1/I_2 ($R^2 = 0.87$). This suggests that the parameters of the JIP test and the DF induction parameters do not contain all the information needed for a precise estimation of the level of desiccation.

4. Discussion

Fluorescence, emitted mainly by PSII antennae chlorophyll *a* molecules, can serve as an intrinsic probe for monitoring the successive steps of excitation energy transformation [79,80]. The variable part of the fluorescence is directly related to the Q_A reduction and it always increases during photoinduced reduction of the quinone acceptor Q_A [81]. As the level of Q_A reduction depends on later stages of energy transformation, the fluorescence signal is sensitive to the overall electron-transfer process. Using the JIP-test approach [56,57], the different steps and phases of the fast PF rise (OJIP-transient) can be linked with the efficiencies of electron transfer in PSII, PSI, and between the two photosystems. In addition to the prompt fluorescence, the PSII antenna chlorophylls also emit delayed fluorescence quanta [82]. Delayed fluorescence intensity is very sensitive to the redox reactions in both the PSII donor and acceptor sides and to the thylakoid membrane energization (for recent review see [68]). The photoinduced kinetics of modulated reflection at 820 nm correspond to the accumulation of $P700^+$, followed by the net re-reduction of $P700^+$ by the intersystem electron carriers [70].

The use of simultaneously measured PF, DF and MR for monitoring the response of the photosynthetic machinery to drying had two goals: first, to examine the sensitivity of different sites of the electron transport chain to drought, and second, to test the sensitivity of the experimental signals to changes in the status of the photosynthetic machinery during desiccation.

In our study we used progressive loss of water in bean plants to induce changes in the photosynthetic reactions. At different levels of desiccation different parts of the linear electron transport were affected. Measuring luminescence and optical characteristics, it was possible to track these changes and relate them to the RWC in the leaf. We found a strong correlation between the measured parameters and RWC which motivated us to develop an automated system — an artificial neural network based on the experimentally determined PD, DF and MR parameters that can determine the RWC in intact leaves.

The shape of the PF induction curve was sensitive to the development of water stress in leaf tissue (Fig. 1A) [76]. The analysis of several parameters of the JIP-test allowed us to localize the drought-induced modifications in the electron transport chain [58]. We found that the redox reactions were strongly affected. The quantum yields of the reactions close to the PSII reaction center were more tolerant to water deficit (Fig. 3A). The three JIP-parameters which reflect the quantum yields of photoinduced electron transfer from P680 to Q_A (φ_{Po}), from Q_A^- to PQ (φ_{Eo}), and from PQ to the PSI electron acceptors (φ_{Ro}), can be arranged according to their decreased sensitivity to water deficit in the sequence $\varphi_{Ro} > \varphi_{Eo} > \varphi_{Po}$. The complex JIP-test parameter, PI_{total} that combines these three parameters and the relative concentration of the reaction center chlorophyll (γ_{Rc}) [57], was sensitive to a wide range of RWC values (Fig. 3B) and is therefore a useful parameter for monitoring stress reactions. On the basis of PI values the Drought Factor Index was introduced [76].

The DF signal provides information about processes in PSII and the photosynthetic membrane in normal and stressed plants [68,83] (including drought stressed plants [58,84]). However such an elaborate model as the JIP-test has not been yet developed for the DF induction curves. In this research we observed that the shape of the DF induction curve was affected by drought (Fig. 1), and moreover the changes started at much lower levels of desiccation than for the PF. It was the fast phase of induction transient of DF – the so called I_1–I_2–D_2 transient (see Fig. 1B) – that best reflected the process of photoinduced closure of PSII reaction centers [77,85]. We demonstrated that the ratio between the two maximums in this DF induction phase almost linearly increased with water loss from fully turgid state down to an RWC of 20% (Fig. 3C).

The yields of PF and DF emissions depended on the water stress in a similar way within the entire RWC range (Fig. 1A and B). They were almost unaffected at RWC above 20% and sharply decreased at lower RWC levels. This implies the existence of a common mechanism of inactivation for both luminescence types, possibly through

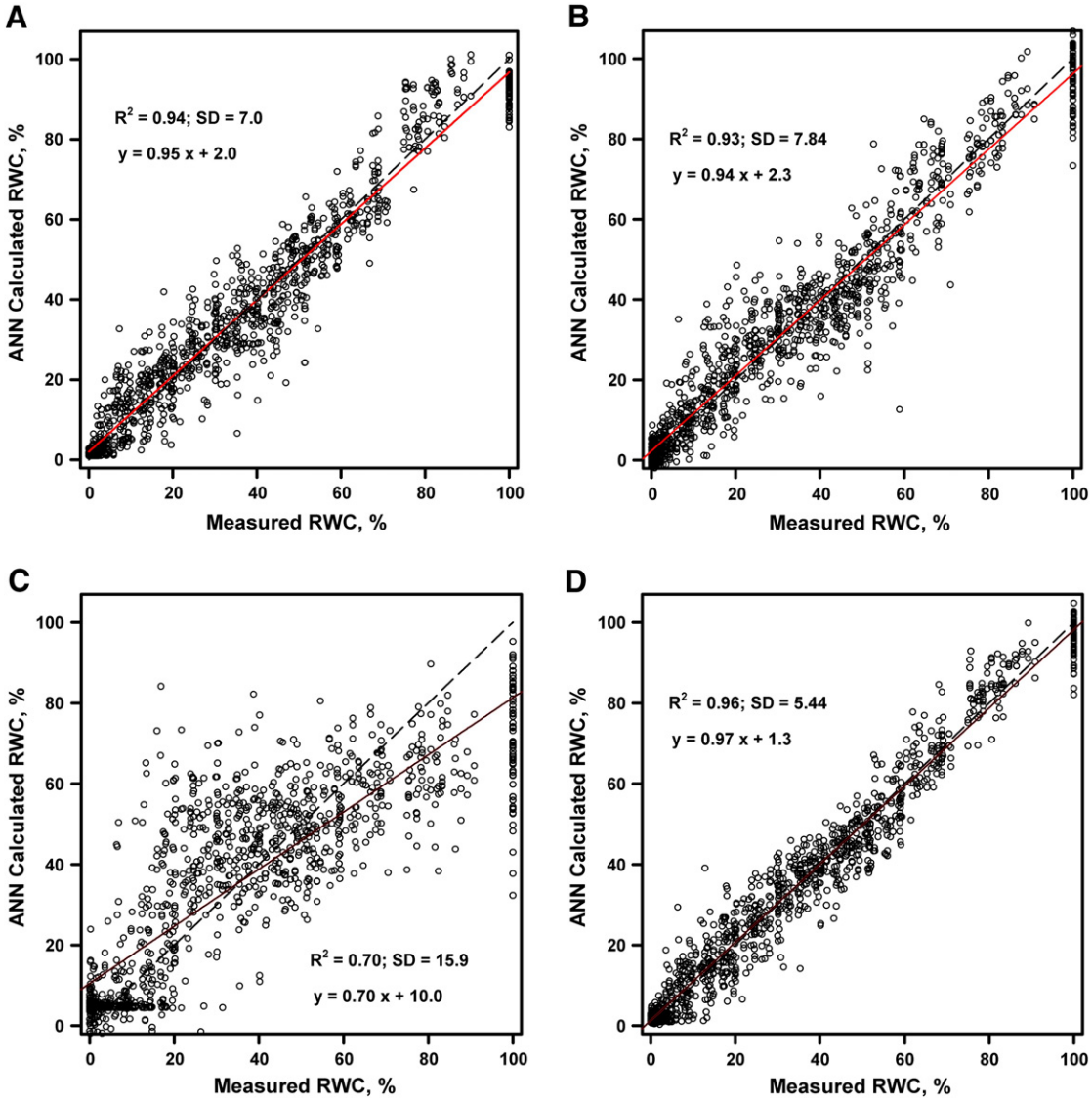

Fig. 4. Results from testing of ANN with three hidden neurons trained with induction curves of PF (A), DF (B) or MR (C) and all three curves used together (D).

the activation of quenchers of the excited states [86] or degradation of chlorophyll molecules [27].

The MR signal was also modified by decreased water content. The fast phase of the signal, which corresponds to the kinetics of the photoinduced changes in P700 redox state [70], was significantly modified only at RWC below 10% (Fig. 3D). The slow phase of the MR signal, which reflects $P700^+$ re-reduction [70], was more sensitive and decreased progressively at RWC values below 30%, disappearing completely at about 3% RWC. We propose that the inactivation of this kinetic phase is manifested as a diminished rate of electron transport through plastoquinone to $P700^+$. The more stable fast phase of the MR signal indicates a higher drought tolerance of the PSI reaction center.

We identified the following successive ranges of specific drought effects:

a) Lowering the RWC to 60% was associated with a decrease in the delayed fluorescence band I_2 compared to I_1 (increase of the ratio I_1/I_2, see Figs. 1B and 3C). As I_2 correlates with electron flow through the PSII acceptor side [77], its decrease indicates a slowdown of the electron flow through PSII. The shape of the PF induction curve remained largely unaffected in the RWC range between 100% and 50%.

b) Lowering RWC from 60% to 20% was accompanied by a linear decrease in φ_{Ro} (Fig. 3A), the loss of the slow growth phase of the MR signal (Figs. 1C and 3D) and the start of the decrease of the overall DF intensity (Fig. 1B). This indicates a suppression of electron transfer from the reduced plastoquinone pool to the PSI reaction center ($P700^+$).

c) At RWC below 15%, the reoxidation of the photoreduced Q_A^- was inhibited which was best monitored by the strong decrease in the parameter φ_{Eo} (Fig. 3A).

d) At RWC under 5%, the parameter φ_{Po} was highly suppressed (Fig. 3A) and the fast phase of photoinduced kinetics of MR signal disappeared (Figs. 1C and 3D). This suggests that at very low water content the primary photochemical reactions in PSI and PSII are inactivated.

Under natural conditions, most plants are subjected to frequent changes in humidity and water availability. As a consequence, plants have evolved various strategies to counteract the problems associated with temporal or spatial water shortage [87]. Such adaptations to drought ensure that the plant maintains relatively stable levels of

photosynthesis, especially in light reactions [58]. For other environmental factors, changes in indices related to the photosynthesis have been successfully used to estimate the severity of stress-induced changes in plants [1,2,4,9]. In contrast, well developed models for photosynthetic rate such as "CO_2 curves" [88] have generally been unsuccessful.

The use of noninvasive techniques for measurements of changes in plant physiology under different stress conditions has considerable practical benefits [1,2,89]. However it is difficult to define robust ecophysiological criteria for estimation of drought sensitivity and potential damage induced by conditions of water scarcity [10]. The reason for this is that while photosynthesis is one of the most sensitive processes to environmental change, photosystems and photosynthetic electron transport are relatively tolerant to changes in water availability [32]. On the other hand, there are many convincing techniques, which are based on fluorescence and optical characteristics, for *in vivo* estimation of changes in electron transport under variation of the environmental conditions.

Our analysis demonstrates that the response of the photosynthetic machinery to drought stress is complex, and is expressed by simultaneous changes in a constellation of parameters calculated from PF, DF and MR signals. The functional state of the photosynthetic apparatus is determined by the water content of the leaf, which as we propose could be described empirically in terms of the pattern of luminescent and optical features. Using pattern recognition methods, a quick, easy and reliable experimental approach for monitoring the physiological state of the leaf could be developed. The feasibility of this approach was demonstrated by the construction of a two-layer artificial neural network which was able to recognize the RWC in a series of "unknown" samples with a correlation between calculated and gravimetrically determined RWC values of about $R^2 \approx 0.98$ (Table 1). Even though this correlation factor seems to be high, the rather large SD value (see Fig. 4 and SD values in Table 1) suggests that there is a relatively high discrepancy between the gravimetrically determined RWC values and the values predicted from the ANN. At the same time, the values of quantum yields of electron transport (Fig. 2A) change together, and their 3D phase diagrams show a relatively narrow trace. We would argue that the observed deviation reflects the heterogeneity of leaf areas in respect to water content, and hence the physiological status of the leaf cell. Thus, some areas of the leaf can locally have higher water content and better physiological status than others — a factor not considered by classical methods for the determination of RWC. If this hypothesis is valid, then RWC determination using ANN is more robust than traditional gravimetric methods.

5. Conclusions

In this work, we demonstrated that chlorophyll fluorescence can be a very informative tool for monitoring water stress effects on the photosynthetic process in plants. We identified four successive specific drought effects over the range of relative water content. First, a decrease in the electron flow through PSII was observed. Second, a suppression of electron transfer from the reduced PQ pool to the PSI reaction center ($P700^+$) was noted. Third, the reoxidation of Q_A^- was inhibited. Finally, there was a suppression of quantum yields of photoinduced electron transport in PSII reaction center to Q_A together with a reduction of the fast phase of photoinduced kinetics of the MR signal.

We were able to precisely plot the desiccation induced changes in the photosynthetic electron transport caused by variations in RWC level. Furthermore, using the multi-signal description on the basis of the experimentally recorded PF, DF and MR signals, we constructed a two-layer artificial neural network as a tool for the determination of water content under *in vivo* conditions. This method could be very reliable for the non-invasive determination of relative water content in intact leaves. However, it should first be validated on intact leaves and under natural drought conditions.

Acknowledgements

This work was supported by Bulgarian National Science Fund, Project No. DO 02-137/15.12.2008. The authors are thankful to Shterian Dambov for his technical assistance in the experimental work.

References

[1] M.H. Kalaji, K. Bosa, J. Koscielniak, Z. Hossain, Chlorophyll *a* fluorescence — a useful tool for the early detection of temperature stress in spring barley (*Hordeum vulgare* L.), J. Integr. Plant Biol. 15 (2011) 925–934.
[2] M.H. Kalaji, Govindjee, K. Bosa, J. Koscielniak, K. Zuk-Golaszewska, Effects of salt stress on photosystem II efficiency and CO_2 assimilation of two Syrian barley landraces, Environ. Exp. Bot. 73 (2011) 64–72.
[3] M.H. Kalaji, S. Pietkiewicz, Salinity effects on plant-growth and other physiological processes, Acta Physiol. Plant. 15 (1993) 89–124.
[4] S.I. Allakhverdiev, Y. Nishiyama, S. Miyari, H. Yamamoto, N. Inagaki, Y. Kanesaki, N. Murata, Salt stress inhibits the repair of photodamaged photosystem II by suppressing the transcription and translation of *psbA* genes in *Synechocystis*, Plant Physiol. 130 (2002) 1443–1453.
[5] S.I. Allakhverdiev, Y. Nishiyama, I. Suzuki, Y. Tasaka, N. Murata, Genetic engineering of the unsaturation of fatty acids in membrane lipids alters the tolerance of *Synechocystis* to salt stress, Proc. Natl. Acad. Sci. U. S. A. 96 (1999) 5862–5867.
[6] B. Barnabas, K. Jager, A. Feher, The effect of drought and heat stress on reproductive processes in cereals, Plant Cell Environ. 31 (2008) 11–38.
[7] F. Loreto, M. Centritto, Leaf carbon assimilation in a water-limited world, Plant Biol. 142 (2008) 154–161.
[8] M.N. Jithesh, S.R. Prashanth, K.R. Sivaprakash, A.K. Parida, Antioxidative response mechanisms in halophytes: their role in stress defence, J. Genet. 85 (2006) 237–254.
[9] S.I. Allakhverdiev, N. Murata, Environmental stress inhibits the synthesis de novo of proteins involved in the photodamage–repair cycle of photosystem II in *Synechocystis* sp. PCC 6803, Biochim. Biophys. Acta 1657 (2004) 23–32.
[10] M.H. Kalaji, T. Loboda, Chlorophyll Fluorescence in Studies of Plants Physiological Status [in Polish], Warsaw University of Life Sciences Press, Warsaw, Poland, 2009.
[11] B. Berger, B. Parent, M. Tester, High-throughput shoot imaging to study drought responses, J. Exp. Bot. 61 (2010) 3519–3528.
[12] P. Lu, W.G. Sang, K.P. Ma, Activity of stress-related antioxidative enzymes in the invasive plant crofton weed (*Eupatorium adenophorum*), J. Integr. Plant Biol. 49 (2007) 1555–1564.
[13] V.D. Kreslavski, R. Carpentier, V.V. Klimov, S.I. Allakhverdiev, Transduction mechanisms of photoreceptor signals in plant cells, J. Photochem. Photobiol. C: Photochem 10 (2009).
[14] B.R. Maricle, D.R. Cobos, C.S. Campbell, Biophysical and morphological leaf adaptations to drought and salinity in salt marsh grasses, Environ. Exp. Bot. 60 (2007) 458–467.
[15] A. Jajoo, A. Kawamori, Anion effects on the structural organization of spinach thylakoid membranes, Biol. Plant. 50 (2006) 444–446.
[16] V. Kreslavski, N. Tatarinzev, N. Shabnova, G. Semenova, A. Kosobryukhov, Characterization of the nature of photosynthetic recovery of wheat seedlings from short-term dark heat exposures and analysis of the mode of acclimation to different light intensities, J. Plant Physiol. 165 (2008) 1592–1600.
[17] P. Ceccato, S. Flasse, S. Tarantola, S. Jacquemoud, J.M. Gregoire, Detecting vegetation leaf water content using reflectance in the optical domain, Remote Sens. Environ. 77 (2001) 22–33.
[18] J. Grace, Plant Water Relations, in: M.J. Crawley (Ed.), Plant Ecology, Blackwell Science, 1997, pp. 28–50.
[19] M. Hassanzadeh, A. Ebadi, M. Panahyan-e-Kivi, A.G. Eshghi, S. Jamaati-e-Somarin, M. Saeidi, R. Zabihi-e-Mahmoodabad, Evaluation of drought stress on relative water content and chlorophyll content of sesame (*Sesamum indicum* L.) genotypes at early flowering stage, Res. J. Environ. Sci. 3 (2009) 345–350.
[20] D.W. Lawlor, G. Cornic, Photosynthesis carbon assimilation and associated metabolism in relation to water deficit in higher plants, Plant Cell Environ. 25 (2002) 275–294.
[21] F. Loreto, N.R. Baker, D.R. Ort, Chloroplast to leaf, in: W.K. Smith, T.C. Vogelmann, C. Cristley (Eds.), Photosynthetic Adaptation, Chloroplast to Landscape, Springer, USA, 2004, pp. 231–261.
[22] M.H. Kalaji, E. Nalborczyk, Gas exchange of barley seedlings growing under salinity stress, Photosynthetica 25 (1991) 197–202.
[23] A.R. Reddy, K.V. Chaitanya, M. Vivekanandan, Drought-induced responses of photosynthesis and antioxidant metabolism in higher plants, J. Plant Physiol. 161 (2004) 1189–1202.
[24] S.K. Singh, K.R. Reddy, Regulation of photosynthesis, fluorescence, stomatal conductance and water-use efficiency of cowpea (*Vigna unguiculata* [L.] Walp.) under drought, J. Photochem. Photobiol. B: Biol. 105 (2011) 40–50.
[25] J. Flexas, J. Bota, J.M. Escalona, B. Sampol, H. Medrano, Effects of drought on photosynthesis in grapevines under field conditions: an evaluation of stomatal and mesophyll limitations, Funct. Plant Biol. 29 (2002) 461–471.
[26] C. Pastenes, P. Pimentel, J. Lillo, Leaf movements and photoinhibition in relation to water stress in field-grown beans, J. Exp. Bot. 56 (2005) 425–433.
[27] C.B. Ahmed, B.B. Rouina, S. Sensoy, M. Boukhris, F.B. Abdallah, Changes in gas exchange, proline accumulation and antioxidative enzyme activities in three olive cultivars under contrasting water availability regimes, Environ. Exp. Bot. 67 (2009) 345–352.

[28] N. Rascio, N. La Rocca, Resurrection plants: the puzzle of surviving extreme vegetative desiccation, Crit. Rev. Plant Sci. 24 (2005) 209–225.
[29] F. Hoekstra, E. Golovina, J. Buitink, Mechanisms of plant desiccation tolerance, Trends Plant Sci. 6 (2001) 431–439.
[30] J. Baker, C. Steele, L. Dure III, Sequence and characterization of 6 LEA proteins and their genes from cotton, Plant Mol. Biol. 11 (1988) 277–291.
[31] P. Berjak, J.M. Farrant, N.W. Pammenter, Seed desiccation-tolerance mechanisms, in: M.A. Jenks, A.J. Wood (Eds.), Plant Desiccation Tolerance, CABI Publishing, Wallingford and New York, 2007, pp. 151–192.
[32] G. Cornic, A. Massacci, Leaf photosynthesis under drought stress, in: N.R. Baker (Ed.), Photosynthesis and the Environment, Kluwer Academic Publishers, 1996, pp. 347–366.
[33] W. Kaiser, Effect of water deficit on photosynthetic capacity, Physiol. Plant. 71 (1987) 142–149.
[34] J. Flexas, J.M. Briantais, Z. Cerovic, H. Medrano, I. Moya, Steady-state and maximum chlorophyll fluorescence responses to water stress in grapevine leaves: a new remote sensing system, Remote Sens. Environ. 73 (2000) 283–297.
[35] W.B. Herppich, D.J. Vonwillert, Dynamic changes in leaf bulk water relations during stomatal oscillations in mangrove species — continuous analysis using a dewpoint hygrometer, Physiol. Plant. 94 (1995) 479–485.
[36] H.G. Jones, R. Serraj, B.R. Loveys, L.Z. Xiong, A. Wheaton, A.H. Price, Thermal infrared imaging of crop canopies for the remote diagnosis and quantification of plant responses to water stress in the field, Funct. Plant Biol. 36 (2009) 978–989.
[37] H.G. Jones, M. Stol, T. Santos, C. de Sousa, M.M. Chaves, O.M. Grant, Use of infrared thermography for monitoring stomatal closure in the field: application to grapevine, J. Exp. Bot. 53 (2002) 2249–2260.
[38] J.U.H. Eitel, P.E. Gessler, A.M.S. Smith, R. Robberecht, Suitability of existing and novel spectral indices to remotely detect water stress in *Populus* spp. For. Ecol. Manage. 229 (2006) 170–182.
[39] H.D. Seelig, A. Hoehn, L.S. Stodieck, D.M. Klaus, W.W. Adams, W.J. Emery, Plant water parameters and the remote sensing R(1300)/R(1450) leaf water index: controlled condition dynamics during the development of water deficit stress, Irrig. Sci. 27 (2009) 357–365.
[40] E.B. Knipling, Physical and physiological basis for the reflectance of visible and near IR radiation from vegetation, Remote Sens. Environ. 1 (1970) 155–159.
[41] N.R. Baker, Chlorophyll fluorescence: a probe of photosynthesis *in vivo*, Annu. Rev. Plant Biol. 59 (2008) 89–113.
[42] H. Kautsky, A. Hirsch, Neue Versuche zur Kohlensaureassimilation, Naturwissenschaften 19 (1931) 964.
[43] E.L. Barsky, S.S. Vasil'ev, V.Z. Paschenko, V.D. Samuilov, Nanosecond fluorescence of chloroplasts as a probe for electron transfer disruption in photosystem II, J. Photochem. Photobiol. B: Biol. 8 (1991) 175–181.
[44] E.M. Aro, I. Virgin, B. Andersson, Photoinhibition of photosystem II. Inactivation, protein damage and turnover, Biochim. Biophys. Acta 1143 (1993) 113–134.
[45] D.R. Shaw, T.F. Peeper, E. Basler, Effect of nitrogen and phosphorus status on the translocation of three herbicides in field bindweed (*Convolvulus arvensis* L.), Plant Growth Regul. 3 (1985) 79–86.
[46] I. Christov, D. Stefanov, T. Velinov, V. Goltsev, K. Georgieva, P. Abracheva, Y. Genova, N. Christov, The symptomless leaf infection with grapevine leafroll associated virus 3 in grown *in vitro* plants as a simple model system for investigation of viral effects on photosynthesis, J. Plant Physiol. 164 (2007) 1124–1133.
[47] A.G. Ivanov, P.V. Sane, V. Hurry, G. Oquist, N.P.A. Huner, Photosystem II reaction centre quenching: mechanisms and physiological role, Photosynth. Res. 98 (2008) 565–574.
[48] Govindjee, W.J.S. Downton, D.C. Fork, P.A. Armond, Chlorophyll *a* fluorescence transient as an indicator of water potential of leaves, Plant Sci. Lett. 20 (1981) 191–194.
[49] M. Havaux, R. Lannoye, Chlorophyll fluorescence induction: a sensitive indicator of water stress in maize plants, Irrig. Sci. 4 (1983) 147–151.
[50] M. Lang, H.K. Lichtenthaler, Sowinska, Heisel, J.A. Meihe, Fluorescence imaging of water and temperature stress in plant leaves, J. Plant Physiol. 148 (1996) 613–621.
[51] J. Schweiger, M. Lang, H.K. Lichtenthaler, Differences in fluorescence excitation spectra of leaves between stressed and non-stressed plants, J. Plant Physiol. 148 (1996) 536–547.
[52] H.K. Lichtenthaler, The stress concept in plants: an introduction, Ann. N. Y. Acad. Sci. 851 (1998) 187–198.
[53] H.K. Lichtenthaler, N. Subhash, O. Wenzel, J.A. Miehe, Laser-induced imaging of blue/red and blue/far-end fluorescence ratios, F440/F690 and F440/F740, as a means of early stress detection in plants, Int. Geosci. Remote Sens. Symp. (IGARSS) 4 (1997) 1799–1801.
[54] J.H. Norikane, K. Kurata, Water stress detection by monitoring fluorescence of plants under ambient light, Trans. Am. Soc. Agric. Eng. 44 (2001) 1915–1922.
[55] N. Subhash, C.N. Mohanan, R.J. Mallia, V. Muralidharan, Quantification of stress adaptation by laser-induced fluorescence spectroscopy of plants exposed to engine exhaust emission and drought, Funct. Plant Biol. 31 (2004) 709–719.
[56] R.J. Strasser, A. Srivastava, M. Tsimilli-Michael, The fluorescence transient as a tool to characterize and screen photosynthetic samples, in: P. Mohanty, Pathre Yunus (Eds.), Probing Photosynthesis: Mechanism, Regulation & Adaptation, Taylor & Francis, London, 2000, pp. 443–480.
[57] R.J. Strasser, M. Tsimilli-Michael, A. Srivastava, Analysis of the chlorophyll *a* fluorescence transient, in: Govindjee Papageorgiou (Ed.), Advances in Photosynthesis and Respiration, Springer, Dordrecht, The Netherlands, 2004, pp. 321–362.
[58] R.J. Strasser, M. Tsimilli-Michael, S. Qiang, V. Goltsev, Simultaneous *in vivo* recording of prompt and delayed fluorescence and 820-nm reflection changes during drying and after rehydration of the resurrection plant *Haberlea rhodopensis*, Biochim. Biophys. Acta 1797 (2010) 1313–1326.
[59] A. Stirbet, Govindjee, On the relation between the Kautsky effect (chlorophyll *a* fluorescence induction) and photosystem II: basics and applications of the OJIP fluorescence transient, J. Photochem. Photobiol. B: Biol. 104 (2011) 236–257.
[60] M. Tsimilli-Michael, R.J. Strasser, *In vivo* assessment of stress impact on plant's vitality: applications in detecting and evaluating the beneficial role of Mycorrhization on host plants, in: A. Varma (Ed.), Mycorrhiza: State of the art, genetics and molecular biology, eco-function, biotechnology, eco-physiology, structure and systematics, Springer, 2008, pp. 679–703.
[61] G. Schansker, S. Toth, R.J. Strasser, Dark recovery of the Chl *a* fluorescence transient (OJIP) after light adaptation: the qT-component of non-photochemical quenching is related to an activated photosystem I acceptor side, Biochim. Biophys. Acta 1757 (2006) 787–797.
[62] R.J. Strasser, The grouping model of plant photosynthesis, in: G. Akoyunoglou (Ed.), Chloroplast Development, Elsevier, North Holland, 1978, pp. 513–524.
[63] R.N. Rad, M.A. Kadir, H.Z.E. Jaafar, D.C. Gement, Physiological and biochemical relationship under drought stress in wheat (*Triticum aestivum*), Afr. J. Biotechnol. 11 (2012) 1574–1578.
[64] A. Porcar-Castell, J.I. Garcia-Plazaola, C.J. Nichol, P. Kolari, B. Olascoaga, N. Kuusinen, B. Fernández-Marín, M. Pulkkinen, E. Juurola, E. Nikinmaa, Physiology of the seasonal relationship between the photochemical reflectance index and photosynthetic light use efficiency, Oecologia (2012), http://dx.doi.org/10.1007/s00442-012-2317-9.
[65] M. Kirova, G. Ceppi, P. Chernev, R.J. Strasser, Using artificial neural networks for plant taxonomic determination based on chlorophyll fluorescence iduction curves, Biotechnol. Biotechnol. Equip. 23 (2009) 941–945 (special Edition).
[66] E. Tyystjarvi, A. Koski, M. Keranen, O. Nevalainen, The Kautsky curve is a built-in, barcode, Biophys. J. 77 (1999) 1159–1167.
[67] A.K. Jain, Algorithms for Clustering Data, Prentice Hall, Englewood Cliffs, NJ, 1988.
[68] V. Goltsev, I. Zaharieva, P. Chernev, R.J. Strasser, Delayed fluorescence in photosynthesis, Photosynth. Res. 101 (2009) 217–232.
[69] I. Zaharieva, V. Goltsev, Advances on photosystem II investigation by measurement of delayed chlorophyll fluorescence by a phosphoroscopic method, Photochem. Photobiol. 77 (2003) 292–298.
[70] G. Schansker, A. Srivastava, Govindjee, R.J. Strasser, Characterization of the 820-nm transmission signal paralleling the chlorophyll *a* fluorescence rise (OJIP) in pea leaves, Funct. Plant Biol. 30 (2003) 785–796.
[71] I. Yordanov, V. Goltsev, D. Stefanov, P. Chernev, I. Zaharieva, M. Kirova, V. Gecheva, R.J. Strasser, Preservation of photosynthetic electron transport from senescence-induced inactivation in primary leaves after decapitation and defoliation of bean plants, J. Plant Physiol. 165 (2008) 1954–1963.
[72] R. Rojas, Neural Networks: A Systematic Introduction, Springer-Verlag, Berlin, Heidelberg, New York, 1996.
[73] G. Hanrahan, Artificial Neural Networks in Biological and Environmental Analysis, CRC Press - Taylor & Francis Group, Boca Raton, FL, 2011.
[74] D.J.C. MacKay, Bayesian interpolation, Neural Comput. 4 (1992) 415–447.
[75] I. Zaharieva, S. Taneva, V. Goltsev, Effect of temperature on the luminescent characteristics in leaves of *Arabidopsis* mutants with decreased unsaturation of the membrane lipids, Bulg. J. Plant Physiol. 27 (2001) 3–18.
[76] M.H. Kalaji, T. Loboda, Photosystem II of barley seedlings under cadmium and lead stress, Plant Soil Environ. 53 (2007) 511–516.
[77] A. Oukarroum, S.E. Madidi, G. Schansker, R.J. Strasser, Probing the responses of barley cultivars (*Hordeum vulgare* L.) by chlorophyll *a* fluorescence OLKJIP under drought stress and re-watering, Environ. Exp. Bot. 60 (2007) 438–446.
[78] C.J. Willmott, Some comments on the evaluation of model performance, Bull. Am. Meteorol. Soc. 63 (1982) 1309–1313.
[79] Chlorophyll *a* Fluorescence: A Signature of Photosynthesis, Springer, Dordrecht, 2004.
[80] V.Z. Paschenko, S.P. Protasov, A.B. Rubin, K.N. Timofeev, L.M. Zamazova, L.B. Rubin, Probing the kinetics of photosystem I and photosystem II fluorescence in pea chloroplasts on a picosecond pulse fluorometer, Biochim. Biophys. Acta 408 (1975) 143–153.
[81] L.N.M. Duysens, H.E. Swears, Mechanism of two photochemical reactions in algae as studied by means of fluorescence, in: P. Japanese Society of Plant (Ed.), Studies on Microalgae and Photosynthetic Bacteria, University of Tokyo Press, Tokyo, 1963, pp. 353–372.
[82] B.L. Strehler, W. Arnold, Light production by green plants, J. Gen. Physiol. 34 (1951) 809–820.
[83] V. Goltsev, I. Zaharieva, P. Chernev, R.J. Strasser, Delayed chlorophyll fluorescence as a monitor for physiological state of photosynthetic apparatus, Biotechnol. Biotechnol. Equip. 23 (2009) 452–457 (Special Edition).
[84] Y. Guo, J. Tan, A kinetic model structure for delayed fluorescence from plants, Biosystems 95 (2009) 98–103.
[85] V. Goltsev, I. Yordanov, Mathematical model of prompt and delayed chlorophyll fluorescence induction kinetics, Photosynthetica 33 (1997) 571–586.
[86] A.G.S. Ivanov, P.V. Sane, V. Hurry, G. Öquist, N.P.A. Huner, Photosystem II reaction centre quenching: mechanisms and physiological role, Photosynth. Res. 98 (2008) 565–574.
[87] W. Ehlers, M. Goss, Water Dynamics in Plant Production, CABI Publ, 2003.
[88] S. von Caemmerer, G.D. Farquhar, Some relationships between the biochemistry of photosynthesis and the gas exchange of leaves, Planta 153 (1981) 376–387.
[89] A. Lavrov, A.B. Utkin, M.J. da Silva, R. Vilar, N.M. Santos, B. Alves, Water stress assessment of cork oak leaves and maritime pine needles based on LIF spectra, Opt. Spectrosc. 112 (2012) 271–279.